

## **PROPOSAL OF THE CRYSTAL EXPERIMENT**

W. Scandale, spokesman of the CRYSTAL  
collaboration

M. Prest, technical coordinator of the CRYSTAL  
collaboration



16<sup>th</sup> of April 2008

# Contents

<b>Executive summary</b>	<b>1</b>
Why . . . . .	1
How . . . . .	2
Who . . . . .	3
Costing profile . . . . .	4
<b>A Crystals for collimation: why and when</b>	<b>7</b>
A.1 What is known on crystals . . . . .	8
A.2 What has already been done . . . . .	10
<b>B The CRYSTAL experiment</b>	<b>17</b>
B.1 Layout and beam requests . . . . .	17
B.2 Materials and costs . . . . .	21
B.3 Time schedule . . . . .	23

# Executive summary

The CRYSTAL experiment intends to assess the possibility of using bent silicon crystals as primary collimators to direct the beam halo onto the secondary absorber thus reducing outscattering, beam losses in critical regions and radiation load.

CRYSTAL has received full support from the LHC Technical Committee on the 30th of January. Four agencies have expressed their interest in the project: CERN, the Russian Institutions (PNPI, IHEP, JINR), INFN (Sections of Ferrara, Legnaro, Milano Bicocca, Roma1) and US LARP (BNL, FNAL, SLAC).

The first version of the MoU is circulating among the collaboration and will be ready to be sent to the funding agencies before the end of April.

This document briefly reviews the CRYSTAL experiment goals, its organization, the cost sharing among the agencies, the needed manpower and the time schedule. Appendix A describes what has already been done with crystals in collimation and why crystals could play a fundamental role while Appendix B analyzes in detail the items summarized in this Executive Summary.

## Why

A collimation system is fundamental to absorb the beam halo for a twofold reason: the limitation of possible damages to the accelerator components and the reduction of the experimental background.

Modern hadron accelerators require the presence of a multi-stage collimation system: the first collimator intercepts the primary beam halo spreading it over the whole solid angle; most of this secondary halo is absorbed by a secondary bulk collimator while scattering creates a tertiary component and the need of a third series of collimators. The primary collimator, which is usually a solid target, has to give to the particle a kick large enough to maximize the impact parameter on the secondary collimator. If this primary collimator were able to deviate the particle outside the beam in a given direction instead of scattering particles on a wide angular range, the cleaning efficiency would increase and the alignment of the

secondary collimator would require a lower precision.

The CRYSTAL experiment will allow to test the possibility of using a bent silicon crystal as a primary collimator. The following deliverables have been identified:

- study of a two stage crystal collimation with the possibility of tracking each single particle with high resolution silicon detectors
- measurement of the cleaning efficiency of each crystal effect (channeling and volume reflection)
- study of the behaviour of a multi-crystal system in order to exploit volume reflection for collimation (which has a higher angular acceptance and a higher deflection efficiency with respect to channeling)
- study of the importance of the multi-turn effect
- development of a highly reliable setup on the SPS ring (consisting of the goniometers in vacuum and the roman pots with single particle tracking detectors) that will allow the test of collimation with crystals, of crystals manufactured with different materials and the possibility of validating simulation and Montecarlo codes

## How

The CRYSTAL experiment will be performed in the SPS LSS5 straight section in storage mode with a low intensity 120 GeV/c proton beam (two other energies will be available, that is 55 GeV/c and 270 GeV/c); the beam will be perturbed to create a diffusive halo as already tested with the RD22 experiment. The experiment will consist of 4 stations:

- the *crystal station* with two goniometers for a multi and a single crystal setup. This station will house also a tracking detector on a linear movement inside the same vacuum tank of the goniometers
- the *first tracking station* located at a phase difference of around 90° with double sided silicon strip detectors for single particle tracking on the channeling and on the volume reflection side
- the *second tracking station* with the same kind of detectors for tracking in the same two directions and with a beam monitor on the vertical side; the two stations will allow to measure x-x' densities and collimation efficiencies with high precision

- the *TAL station* with the tungsten secondary collimator

The observables of the experiment are the collimation efficiencies, the measurement of the phase space and of the cleaning efficiency through the losses along the ring.

## Who

CERN and three agencies (INFN, US LARP and the Russian Institutions) have stated their official interest in participating to the CRYSTAL experiment and in contributing to its setup and running. Fig. 1 presents the organization chart of the experiment.

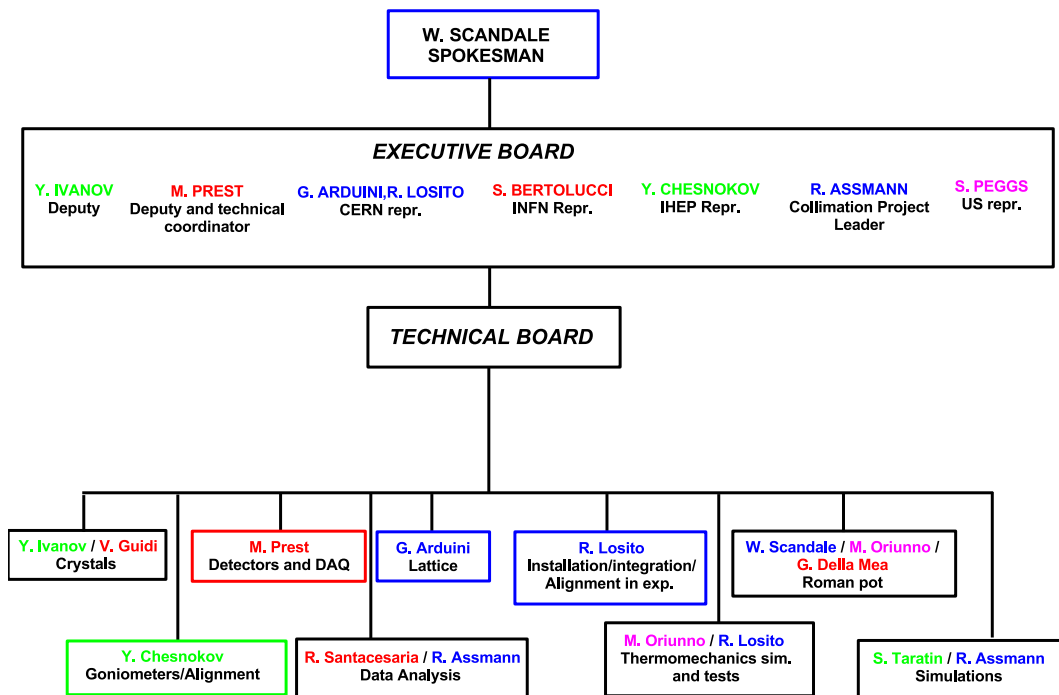


Figure 1: Organization chart. Colours refer to different agencies: blue for CERN, green for Russian Institutions, red for INFN and violet for US LARP.

The CRYSTAL organization foresees an *Executive Board* with representatives from all the institutions, the spokesman, his deputies and the technical coordinator

and a *Technical Board* with the representatives of the working groups. The total number of participants is 55.

The external agencies have guaranteed an at-home manpower contribution of 25 Full Time Equivalent per year (the project will last two years, 2008 and 2009). The CERN support (that can be estimated in 1 FTE) will be required for all the details concerning the machine (design, infrastructure, controls, installation) with a dedicated effort concentrated in 2009.

## Costing profile

The experiment will use part of the instrumentation already developed for the RD22 collaboration (the goniometers and the vacuum tank) and for the TOTEM collaboration (the roman pot used in the TOTEM tests on the SPS in 2004).

As far as costs are concerned, the refurbishing of the goniometers and of the roman pots will be shared between CERN and the other funding agencies, the cabling and infrastructure costs will be in charge of CERN while the crystal and diagnostic systems will be completely in charge of the other funding agencies.

The overall cost of the experiment is 1176 kCHF to which a 360 kCHF equivalent should be added for the already existing infrastructures and for developments financed under other projects. CERN will contribute to 25% of the real cost (39% with respect to the total) while in the remaining 75% (61%) also the travelling and per diem costs are included.

Tab. 1 shows the contributions of the agencies on the different items of the project, both in absolute terms and in percentage (considering the overall cost of 1536 kCHF).

Tab. 2 presents the effective and total costs for CERN and tab. 3 the breakdown for the CERN contribution. In our present view, the 300 kCHF would be shared among the AT (130 kCHF) and the AB (170 kCHF) division; as far as the manpower is concerned, AT would contribute with 0.2 FTE (plus the person of Walter Scandale) and AB with 0.8 FTE.

All the hardware will be tested and ready to be installed in the SPS for the end of 2008, in order to perform and conclude the experiment before the end of 2009.

Item	Cost (kCHF)	CERN	INFN	RUSSIA	US-LARP
Crystal station	500	240 (48%)	60 (12%)	200 (40%)	- -
Tracking stations	207×2	150 (36.4%)	187 (45.4%)	- -	75 (18.2%)
Spare tracking and upgrade	116	- -	- -	- -	116 (100%)
Design, install., data taking	508	210 (41.3%)	139 (27.4%)	100 (19.7%)	59 (11.6%)

Table 1: Overall costs and absolute and percentage contributions of the four agencies.

Item	Effective cost (kCHF)	Total cost (kCHF)
Crystal station	85	240
Tracking stations	85	150
Spare tracking and upgrade	-	-
Design, install., data taking	130	210
Total	300	600

Table 2: Effective and total costs for CERN; the “design” item includes also the contingency of 70 kCHF.

Item	Single items	Effective cost (kCHF)	Cost equivalent items	Cost (kCHF)	Total cost (kCHF)
<b>Crystal station</b>		<b>85</b>		<b>155</b>	<b>240</b>
	Control electronics for the goniometer	25	Vacuum tank	35	
	Near crystal detector movement	30	Goniometers	70	
	Vacuum flanges and pipes	30	Cabling	50	
<b>Tracking stations</b>		<b>85</b>		<b>65</b>	<b>150</b>
	Control electronics for roman pots	15	Existing roman pot	35	
	Cabling	20	Cabling	30	
	Vacuum flanges and pipes	50			
<b>Design, install., data taking</b>		<b>130</b>		<b>80</b>	<b>210</b>
	Design	60	infrastructure (racks,crates, computing, control room)	80	
	Contingency	70			
<b>Total</b>		<b>300</b>		<b>300</b>	<b>600</b>

Table 3: Breakdown of the costs for the CERN contribution.



# Appendix A

## Crystals for collimation: why and when

As already underlined in the Executive Summary, collimators are fundamental to absorb the beam halo both for the life of the accelerators (especially in modern hadron accelerators due to their use of superconducting magnets) and for the physics of the experiments.

Fig. A.1(a) shows a traditional multistage collimation system consisting of an amorphous target that spreads the primary halo creating a secondary one that has to be intercepted by the second stage of the collimation system.

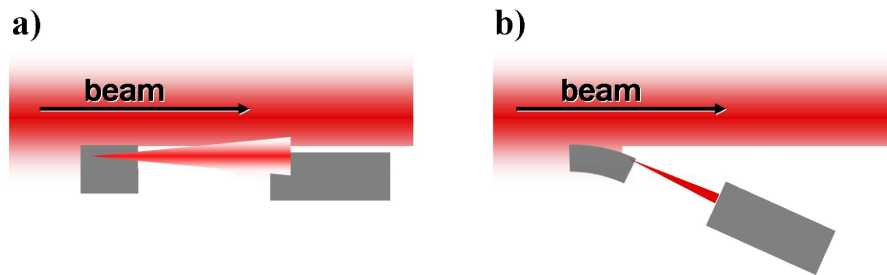


Figure A.1: a) Traditional multistage collimation system: an amorphous target spreads the primary halo so that most of it can be intercepted by a (more distant with respect to the beam) secondary collimator. b) Crystal based collimation: a bent crystal steers (through channeling) the primary halo into an absorber.

Fig. A.1(b) shows a possible alternative to a standard primary collimator, that is a system able to deviate the particles outside the beam in a given direction thus increasing the cleaning efficiency and loosing the requirement on the precision of the alignment of the secondary collimator.

This is exactly what a bent crystal would do.

The story of crystals in high energy physics dates almost one century ago. In 1912, J. Stark [1] suggested that certain directions in a crystal could be more transparent to charged particles with respect to amorphous materials. This idea was put in stand by till the '60s when several experiments demonstrated the unusual penetration of ion beams in crystals. It was just like opening a door on the future: from there on, crystals have been intensively studied at low energies. Then in 1976, E. N. Tsyganov [2] proposed to bend a crystal to deflect a high energy beam; the idea was experimentally proven in 1979 at Fermilab.

In the following sections, a brief review of the phenomena connected with the passage of charged particles in crystals is presented (section 1) together with the main measurements performed around the world to understand both the physics of crystals and their role in collimation (section 2).

## A.1 What is known on crystals

When a charged particle crosses a solid amorphous target, it collides with the atoms of the target itself losing energy and undergoing scattering. When the target material is monocrystalline, depending on the alignment with respect to the crystal lattice, the particle could experience a coherent scattering with the atoms of the crystal itself. If the particle is aligned, within a small angle, to a crystal plane (axis) its interaction with the atoms of the plane (axis) is described by an average continuous potential generated by them [3] which increases approaching the plane where the nuclei are placed, as shown in fig. A.2(a). The electric field of two neighbouring planes forms a quasi harmonic potential well (fig. A.2(b)) which is able to trap positive charged particles in between the atomic planes.

This phenomenon is called planar channeling and takes place when the particle kinetic energy in the transversal direction with respect to the plane is smaller than the maximum value of the interplanar potential. In other words the angle between the particle trajectory and the crystal plane should not overcome a critical value,

called Lindhard angle expressed as  $\theta_L = \sqrt{\frac{2E_c}{pv}}$ , where  $E_c$  is the maximum value

of the interplanar potential and  $p$  and  $v$  are the particle momentum and velocity. For the (110) orientation in a silicon crystal,  $E_c$  is about 16 eV, which gives  $\theta_L \simeq 10 \mu\text{rad}$  at 400 GeV/c.  $\theta_L$  decreases as the square root of the particle energy while the multiple scattering, which is the channeling effect competitor, goes as the inverse of the energy; thus the channeling effect will be more evident as the particle energy increases.

The confinement power of the crystalline planes can be exploited to deviate the trajectory of the channeled particles, using a bent crystal. Fig. A.3(a) shows the

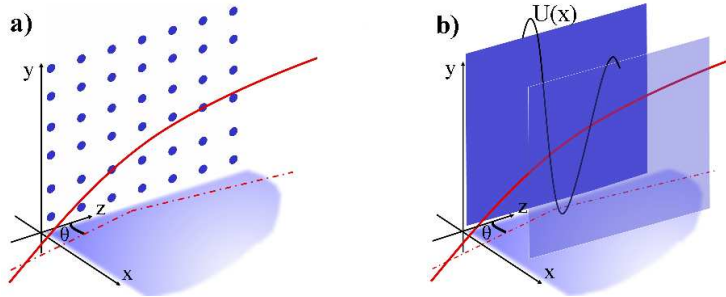


Figure A.2: a) A particle trajectory in a crystal misaligned with respect to the axis but at a small angle with respect to the crystalline plane, placed in the  $z - y$  plane. b) The particle experiences an average potential due to the planes ( $U(x)$ , represented by the black line).

scheme of a bent crystal; a channeled particle oscillates in the channel following the crystal curvature reaching a final deviation of  $\theta_C = l/R$  where  $l$  is the crystal length and  $R$  the curvature radius. The effect of the bending can be described by the replacement of the atomic interplanar potential with an effective one, which takes into account the centrifugal force. This force lowers the interplanar potential barrier and the critical angle of a factor  $(1 - R_c/R)$  where  $R_c$  is the critical radius, which indicates the minimum curvature radius that allows channeling;  $R_c$  is proportional to the particle energy and its value is about 80 cm in silicon at 400 GeV/c.

Fig. A.3(b) schematically shows the effective potential resulting from the combi-

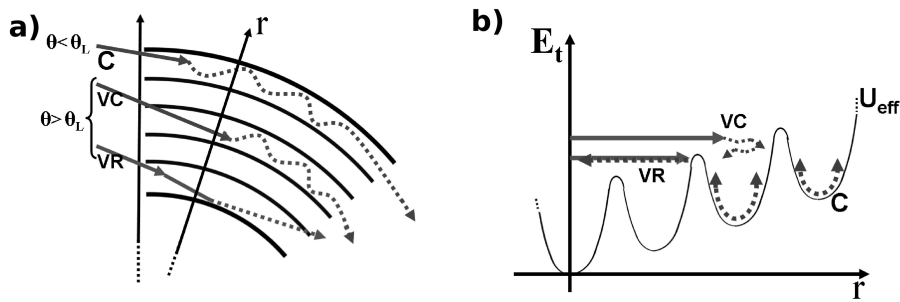


Figure A.3: a) A schematic view of a bent crystal. b) The effective crystal potential is the sum of the centrifugal force and the interplanar potential. The arrows indicate the particles trajectories corresponding to: channeling (C), volume capture (VC), volume reflection (VR).

nation of the interplanar electric field and the centrifugal force. The arrows indi-

cate the possible particle trajectory in the bent crystal: *channeling* (C) takes place if the particle incoming angle, with respect to the crystal planes, is smaller than the Lindhard one; when this angle overcomes the critical value the tangency point between the particle trajectory and the crystalline planes moves inside the crystal (in its volume) where the particle can be either captured in the channel (VC) or reflected by the interplanar potential (VR). The *volume capture* takes place when the particle, which is almost aligned with the channel direction inside the crystal, loses part of its transversal energy, due to the scattering with nuclei and electrons, so that it is trapped in the channel. The capture probability is proportional to  $\theta_L$  and to the scattering yield and it goes as  $E^{-3/2}$ , where  $E$  is the particle energy. The particles which are not captured are reflected by the potential barrier of an angle which depends on the curvature radius and on the particular particle trajectory and in average corresponds to  $1.5\theta_L$ . The *volume reflection* effect has been discovered in computer simulations [4] and observed for the first time in [5]; although the reflection angle determined by the beam energy and the crystal material is small, the high efficiency and angular acceptance make this effect interesting for beam collimation.

Another phenomenon, the *dechanneling*, completes the list of the possible effects in a bent crystal: it concerns particles which are initially channeled but escape from the interplanar potential because of the fluctuations of the transversal kinetic energy (due to scattering); in practice it is the opposite of volume capture.

## A.2 What has already been done

Following Tsyganov's idea, bent crystals have become an efficient tool for steering high energy particles at accelerators: they are easy to use and compact, their behaviour is predictable and reliable and they have been demonstrated to be rad-hard [6]. They can be used for particle extraction [7], for focusing [8] and splitting [9] the beam; moreover crystal undulators are being studied to produce high intensity photon beams [10].

Up to the dawn of the 21<sup>st</sup> century, the most exploited crystal feature has been channeling: the Fermilab experiment [2] measured a channeling efficiency of 1% which jumped to 10-20% in 1996 in a SPS extraction experiment [11], thanks to the multi-turn effect [12]. The multi-turn effect takes place in a circular accelerator where the particles stay on the same orbit for many turns. When the crystal is put in the beam halo with the correct orientation for channeling and a particle crosses it without being channeled, the particle has anyway a new possibility of being channeled the next turn and so on. The reduction of the crystal size in the beam direction increases the average number of particles crossings and thus the channeling efficiency. The multi-turn effect theory generated another burst of ac-

tivity on one hand for the understanding of crystal behaviour (mainly at IHEP) and on the other one for a real application of collimation of very high energy beams (RHIC and Tevatron).

The Institute of High Energy Physics has several locations on the U-70 synchrotron ring where crystals are installed and used routinely for extraction and collimation studies. Fig. A.4(a) presents the extraction efficiencies measured in a series of experiments in the period 1997-2000 as a function of the crystal length along the beam compared with the Montecarlo simulation, while fig. A.4(b) shows the collimation efficiency as a function of the acceleration energy of the U-70 ring compared with the Montecarlo prediction.

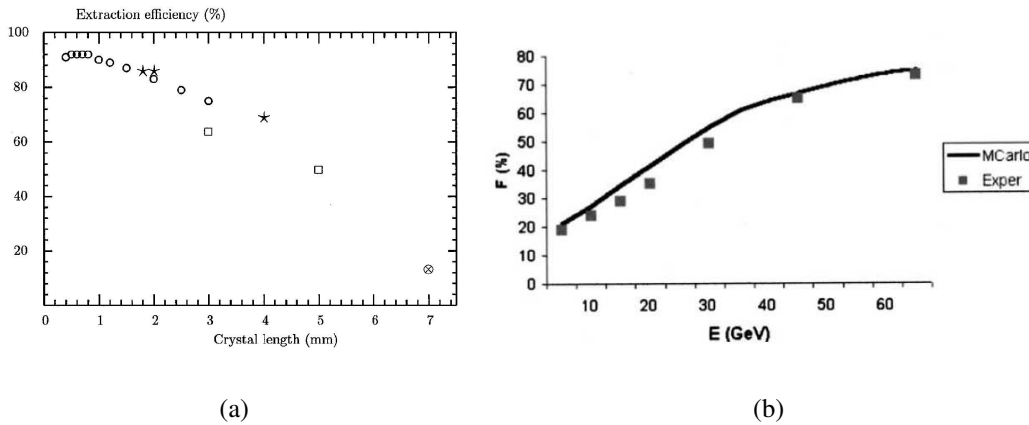


Figure A.4: (a) Crystal extraction efficiency for 70 GeV protons as a function of the crystal length: IHEP measurements ( $\star$ ,  $\otimes$  for strip crystals; box for an O-shaped crystal) and Montecarlo predictions ( $\circ$ ). (b) Crystal collimation efficiency measured during the acceleration phase of the U-70 ring compared with the Montecarlo prediction.

From 2001, two significant crystal collimation experiments took place at RHIC (with gold ions) and at the Tevatron (with protons of 980 GeV/c) accelerator. They used the same crystal (fig. A.5, an O-shaped crystal from PNPI 5 mm long in the beam direction, 1 mm wide and with a bending angle of 440  $\mu$ rad) and an equivalent method to check the results. Moreover, being the tests devoted to the increase of the accelerator performance reducing the experimental background, they needed to receive immediate feedback from the running experiments.

Fig. A.6(a) presents the measurement setup [13]: a bent crystal was installed in one of the RHIC rings as the first stage of a two collimator system; the crystal angle in the horizontal plane was changed by a piezoelectric inchworm pushing the lever arm at whose end the crystal was mounted. The data taking procedure

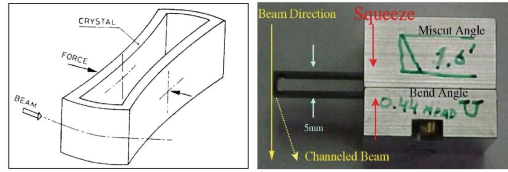


Figure A.5: Scheme of the O-shaped crystal bending mechanism (left); photo of the crystal mounted on its holder (right).

was the following: the crystal was inserted and the scattering of the halo particles was detected by a set of upstream PIN diodes; the crystal was rotated in steps with respect to the beam direction; during the crystal rotation, the beam loss rate was kept under control. Fig. A.6(b) shows an example of a scan as monitored by a PIN diode: the drop in the curve indicates channeling in the crystal; the channeling efficiency is computed dividing the depth of the channeling dip by the background rate and gives 25%, a very high value with respect to the 11% obtained at the SPS with Pb ions [14]. The blue curve in fig. A.6(b) is obtained using the design parameters for the phase space while the red one takes into account a rotation of the phase space ellipse explaining why the reached collimation efficiency is a factor 2 lower than what expected. The experimental background was measured

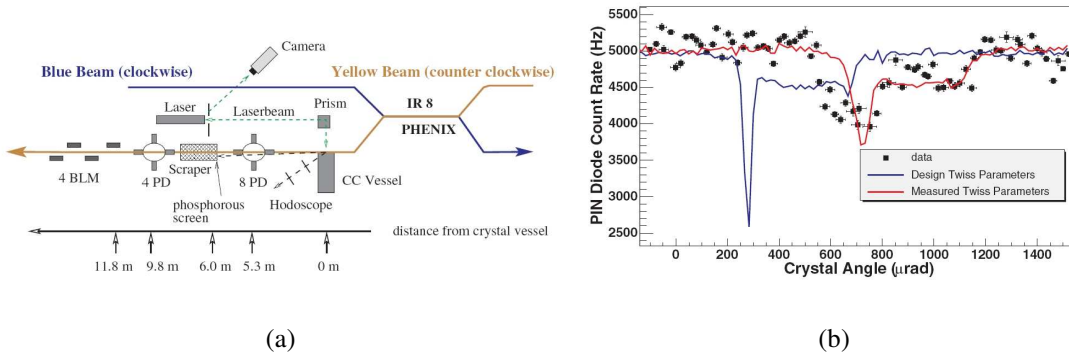


Figure A.6: (a) The RHIC crystal collimation setup. (b) Comparison between the RHIC data and the Montecarlo predictions.

by the STAR detector but the result was negative [15] due probably to the lower channeling efficiency reached in the position where the crystal was located; this unsuccessful measurement demonstrated how the beam optics should be adjusted at the crystal location in order to have a small beam divergence at the crystal entry face to match the crystal channeling angular acceptance (which is fixed by the

crystal features).

In 2005 the same crystal on the same goniometer was installed at the Tevatron accelerator in a straight section where it replaced a tungsten primary collimator [16]. Fig. A.7 shows the experimental layout. Fig. A.8(a) presents the results in

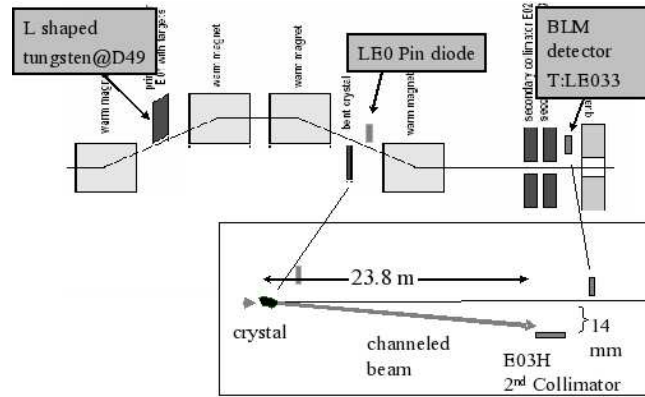


Figure A.7: Layout of the experimental setup at the Tevatron accelerator.

terms of the crystal angular scan (as in the RHIC case) compared with the Monte-carlo simulation while fig. A.8(b) shows the background level at the CDF and D0 experiments before and after the insertion of the crystal as a primary collimator: the background has been reduced of a factor 2.

In 2006, another big breakthrough took place: the H8RD22 collaboration observed for the first time the volume reflection phenomenon with a high energy (400 GeV/c) proton beam [17] (the observation at low energy had already been performed [5, 18]).

The crystal was positioned in the beam and aligned thanks to a goniometric system characterized by a precision one order of magnitude higher than the Lindhard critical angle (around  $1 \mu\text{rad}$ ). The particle tracks were reconstructed with high resolution silicon strip detectors [19]. Fig. A.9 presents the angular scan of a strip crystal (INFN Fe): the angular profile of the crystal is plotted as a function of the goniometer angle. The following crystal effects can be identified:

1. the crystal is misaligned and behaves as an amorphous material (start and end of the plot along the x axis)
2. the crystal is aligned and the channeling peak appears (bottom of the plot, with a deflection angle of  $157.6 \pm 0.2 \mu\text{rad}$ , which, taking into account the crystal length of 3 mm, is equivalent to a magnetic field of about 72 T);

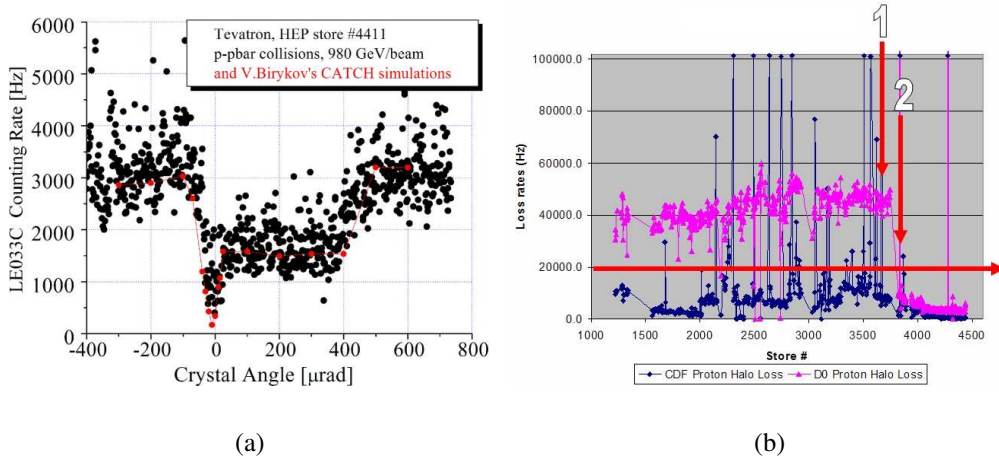


Figure A.8: (a) Crystal angular scan: scattering rate as a function of the crystal angle with respect to the beam direction; the red points are the Montecarlo prediction. (b) Proton halo rate recorded by CDF and D0. The horizontal line represents the proton halo loss limit while the vertical ones indicate the machine developments performed to reduce the experimental background: 1) the installation of a double scraper; 2) the improvement of the vacuum system and of the alignment and the installation of the crystal collimator.

the region between the main peak and the channeling one is filled with the dechanneled particles

- the angle between the crystal and the beam is larger than the Lindhard one and the beam is reflected on the opposite side with respect to channeling (with an angle of  $13.8 \pm 0.1 \mu\text{rad}$ ); the diagonal region connecting the channeling peak and the end of the reflection region is filled by volume captured particles.

The measured reflection efficiency is  $98.25 \pm 0.13\%$ , while the channeling one is  $51.18 \pm 0.72\%$ .

The first data taking of the H8RD22 collaboration confirmed that the channeling angular acceptance is limited by the Lindhard critical angle ( $\simeq 10 \mu\text{rad}$  at 400 GeV/c); the volume reflection angular acceptance, on the other hand, roughly corresponds to the channeling deflection angle and therefore is larger than the channeling one (in this case it is about  $130 \mu\text{rad}$ ). A large angular acceptance makes the crystal alignment easier and the deflection efficiency almost independent from the beam divergence.

Thanks to its larger angular acceptance and efficiency, the volume reflection could represent an interesting alternative to channeling for beam steering applications



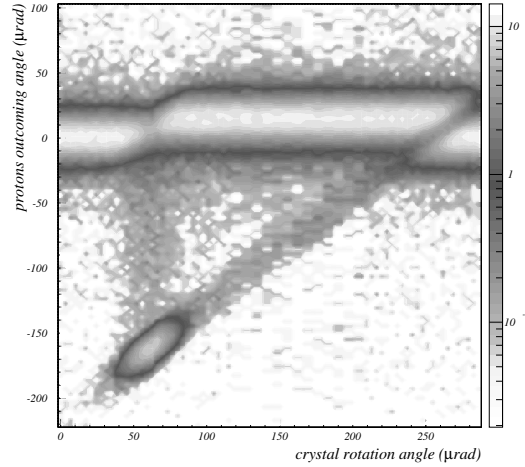


Figure A.9: Angular scan of the ST4 crystal. The beam angular profile is plotted as a function of the goniometer angle. The grey code represents the intensity in a logarithmic scale.

in high energy physics such as beam collimation. To overcome the difficulty of a fixed and small deflection angle, a multireflection system composed of many crystals has also been studied [20]. This system should multiply the reflection angle with a small decrease in efficiency. Fig. A.10(a) shows the first successful multireflection attempt: two quasimosaic crystals (PNPI) have been aligned and placed on the goniometer. The plot shows the result of the angular scan where two almost overlapped channeling peaks are visible on the left side while in the central region the double reflection is present. Fig. A.10(b) compares a frame of the scan in double reflection (grey plot) with an amorphous one (white plot); the deflection angle is  $23.4 \pm 0.4 \mu\text{rad}$  and the deflection efficiency is  $95.7 \pm 0.4\%$ .

In October 2007, another step forward has been made, aligning 5 quasimosaic crystals remotely with piezoelectric motors. Fig. A.11 shows the resulting angular scan. The deviation angle is 5 times the single crystal one with an efficiency of the order of 90%.

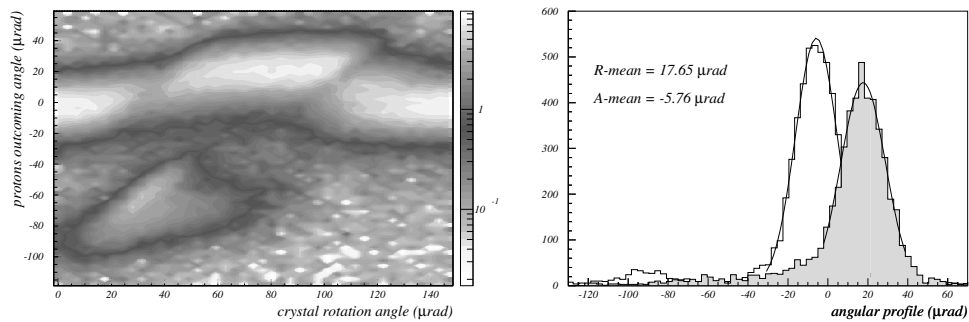


Figure A.10: (a) Angular scan of two aligned quasimosaic crystals. The beam angular profile is plotted as a function of the goniometer angle; the grey code represents the intensity in a logarithmic scale. (b) The comparison between a profile of both crystals in the amorphous orientation (white) and a profile in which they are both in reflection; the total deflection angle doubles the single reflection one.

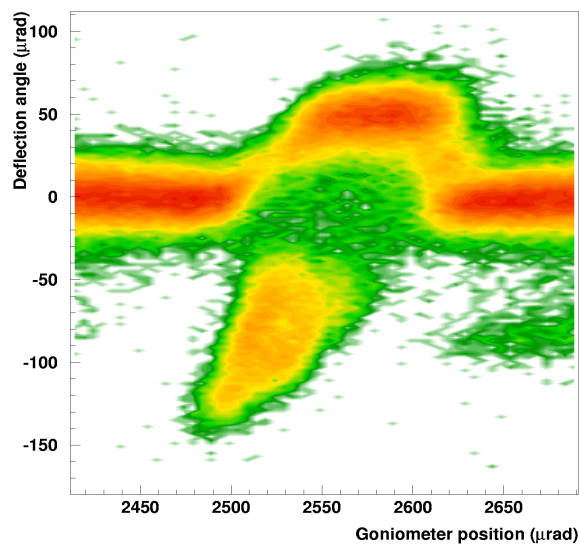


Figure A.11: Angular scan of 5 aligned quasimosaic crystals. The crystals have been aligned with piezoelectric motors; data have still to be published.

# Appendix B

## The CRYSTAL experiment

This appendix describes in detail the CRYSTAL experiment.

The final layout is still in the definition phase; in particular the positions of the second roman pot and the TAL collimator have to be decided accordingly with the simulation results.

The refurbishing of the crystal station and the prototyping of the tracking stations have already started in order to be ready for a dry run in October 2008 on the SPS H4 line.

The crystal ensembles for the SPS will be tested on the SPS H8 line starting from the second half of August.

### B.1 Layout and beam requests

The experiment will be located in the LSS5 straight section of the 5<sup>th</sup> sextant (fig. B.1). It will consist of 4 stations:

- the *crystal station*: it consists of two crystals mounted on two goniometers (one for the multi-crystal setup and one for the single crystal) in the vacuum tank located upstream of QF51810. The two goniometers are being refurbished by PNPI as far as the mechanical and the control parts are concerned; two new goniometers are being designed by IHEP in order to allow the test of more crystals. A dedicated alignment system will be designed (IHEP), able to check the alignment status in real time also during the data taking.
- the *first tracking station*: it consists of a roman pot located in the next cell with respect to the goniometer (at a distance of around 50 m from the goniometer, that is at a phase difference of 90° to maximize the distance of the steered particles from the beam core). This station will allow the monitoring/tracking in two directions (right and left, that is on the volume reflection

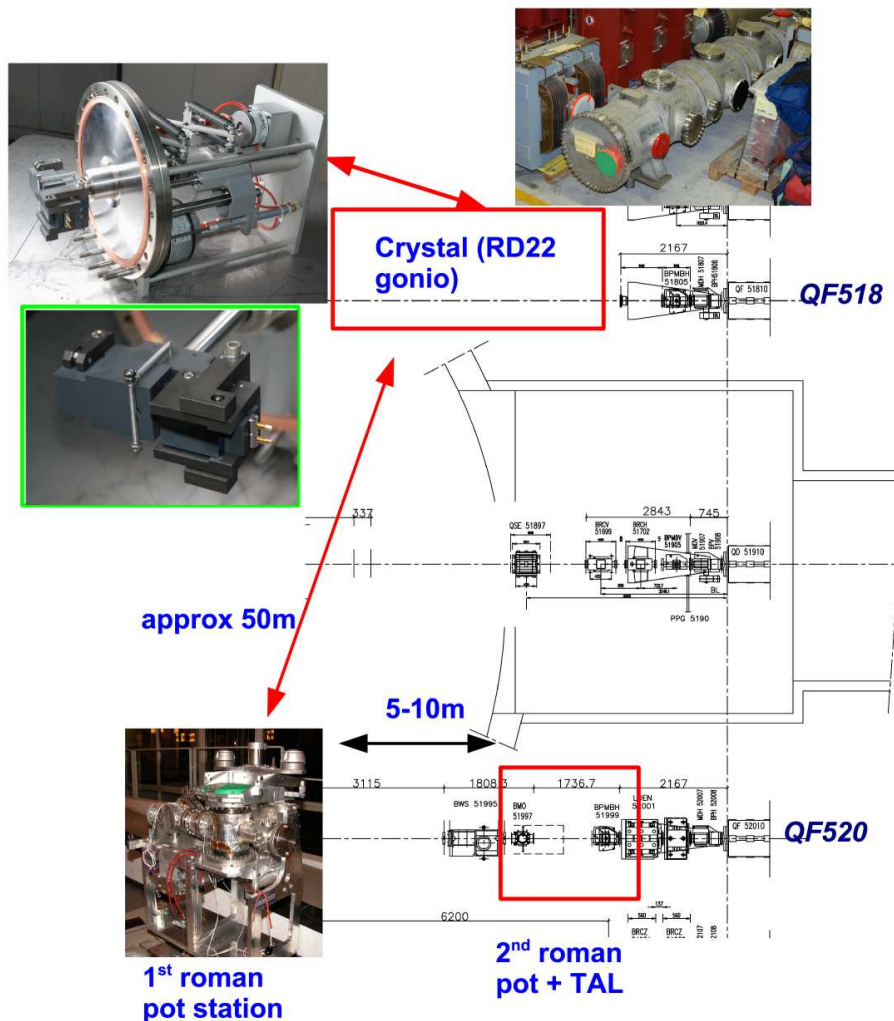


Figure B.1: Possible layout for the CRYSTAL experiment on the SPS; the photos in the insert show the RD22 goniometer (top left), the RD22 vacuum tank (top) and the roman pot (bottom left).

and on the channeling side). All the tracking detectors are double sided silicon strip detectors (with a readout pitch of  $50 \mu\text{m}$ , produced by FBK-Italy) readout by low noise self triggering ASICs.

- the *second tracking station*: it consists of a roman pot located as far as possible from the previous one and before the secondary collimator; it will be equipped with the second tracking system and a vertical monitoring. The vertical detector is a single side detector readout by the Mythen2 ASICs

(PSI). The two tracking stations will allow to measure completely the phase space.

- the *TAL station*: it consists of a tungsten secondary collimator; the two tracking stations will allow to reconstruct each single track entering this collimator both with and without the crystal. In this way,  $x$ - $x'$  densities and collimation efficiencies will be measured with high precision. The TAL and the second tracking station will be located just upstream of QF52010.
- the distributed system of beam loss monitors present along the SPS circumference will be used to check that the halo is lost only in the crystal location and nowhere else.

The possibility of having a silicon detector with a small dead region not inserted in a roman pot but on a dedicated movable station near the crystal is being investigated. The silicon detector will be protected against the electromagnetic interference with a thin layer of aluminum (probably sputtered on a mylar or similar support). This detector will allow to study the multi-turn effect for collimation and to compute the efficiency as the ratio between the number of particles impinging on the crystal and steered by the crystal itself (as measured by the roman pot detectors) on a single turn basis.

The silicon detectors will be connected to the frontend electronics via a flexible fanout in order to position the electronics as far as possible from the beam. Three different types of ASICs will be used:

- the VATAGP (Gamma Medica, Norway) for the near crystal detector; it is a 128 channel ASIC with self triggering capabilities and a sparse readout system.
- the VA1TA (Gamma Medica, Norway) for the tracking detectors; it is a 128 channel ASIC with a double shaper: a fast one (75 ns) for the trigger generation and a slow one (tunable between 0.3 and 1  $\mu$ s) for the analog readout.
- the Mythen2 (PSI) for the profilometer; it is a 128 channel ASIC with counting capabilities and a maximum rate per channel greater than 3 MHz.

The first 2 ASICs are built in 0.35  $\mu$ m N-well CMOS double-poly triple-metal technology and preliminary measurements show they can stand up to 20 Mrad; the Mythen2 ASIC is built in 0.25  $\mu$ m, that is intrinsically radiation hard. Tests to confirm these numbers are foreseen.

The readout electronics will be located outside the roman pot and will be a copy of the one developed for the new data taking at the H8 beamline (ADC with the

FPGA for a high speed readout); the absence of a spilled structure will require the implementation of a two stage storage in order to store data while transferring them to the PC without introducing dead time. Depending on the occupancy of the detectors and the possible pile-up, work is being done to allow a maximum data rate of 100 kHz.

The beam features will be the following:

- proton coasting beam of 120 GeV/c (but also 55 GeV/c and 270 GeV/c will be available).
- maximum halo flux compatible with a DAQ rate of 25 kHz but work is being done to increase this number to 100 kHz; a dedicated study will be performed to determine the fraction of multi-particle events and the capability of a two-station setup to reconstruct multi-particle tracks; as far as the counting electronics is concerned, the DAQ rate is at least 3 MHz per strip. The tracking systems will be synchronized among them and with the goniometer movement.
- the beam halo will be created applying random horizontal kicks given by the electrostatic deflector plates of the SPS damper system through an external generator of bandwidth limited white noise. This noise sums up to a series of uncorrelated random kicks making the particles diffusing towards the crystal. This technique has already been successfully used for RD22.

The halo will be intercepted at around  $6 \sigma$  from the beam core ( $1 \sigma = 0.71$  mm at  $\beta_{max}$ ; if the particle population were too low, the crystal will be moved towards the  $3 \sigma$  region). Locating the tracking system in a region with a phase difference of around  $90^\circ$  and considering a steering angle for the volume reflection of  $100 \mu\text{rad}$  (given by the one measured on the October H8 testbeam with 400 GeV/c protons and by the fact that it is foreseen to run at 120 GeV/c) a horizontal displacement of the particles of 3.6 mm has been simulated.

The following beamtime has been requested:

- 3 shifts to setup the beam
- 5 to 6 periods of 2/3 shifts in distinct blocks to test the crystal in collimation mode
- 1 to 2 periods of 2 shifts in distinct blocks to test the crystal in high flux.

## B.2 Materials and costs

Fig. B.2 presents a detailed breakdown of the costs of the experiment, while fig. B.3 shows the cost profile for the 4 Institutions over the 2 years of the project. The following has to be taken into account:

- the table considers both the effective costs of the experiment and the cost equivalent of the already existing infrastructures/hardware items (such as the vacuum tank, the goniometers, the roman pot, part of the cables) or the developments that have been financed under other projects (such as the INFN contribution for the crystals in the framework of the NTA program). These items are indicated in blue in the table and the relative total is computed in a separate column
- the table considers the assembly and test of several spares of the tracking modules with a more performing frontend electronics. These modules will be prepared starting at the end of 2008 in order to improve the setup performance in a possible later run (as indicated in the Executive Summary, one of the deliverables is a fail proof setup to test crystals manufactured with other materials and to validate simulation and Montecarlo codes). The spare production is fully covered in terms of costs by the US part of the collaboration, while the effective work will be performed and followed by INFN
- the installation/data taking contribution from the agencies other than CERN consists in the costs of maintaining manpower with the adequate expertise at CERN in all the needed periods. No cost evaluation has been performed on the analysis needs (computers, farms, storage and so on; the computing item listed in the infrastructure refers to the data acquisition) leaving this item under each Institution responsibility
- some of the items under the “infrastructure” category are still under investigation: the already available cables for the goniometers, the roman pots and the signal cables for the detectors (whose length depends on the experimental layout), crates and racks for the instrumentation, the vacuum parts (flanges and pipes)

<i>ITEM</i>	<i>CERN</i>	<i>INFN</i>	<i>RUSSIA</i>	<i>USA</i>	<i>TOTAL</i>	<i>Cost eq. for existing parts</i>
<b>DETECTORS</b>		<b>110</b>		<b>108</b>	<b>218</b>	
ASICs		36		53		
Silicon		9				
Frontend		21		15		
Assembly		13		16		
Mechanics		16		16		
Test systems		15		8		
<b>READOUT</b>		<b>32</b>		<b>8</b>	<b>40</b>	
SOC/ADC/VME boards		16		8		
Cables and power supplies		16				
<b>ROMAN POTS</b>	<b>15</b>	<b>45</b>		<b>75</b>	<b>135</b>	<b>35</b>
Existing roman pot	35					
Existing roman pot modification		15				
New roman pot with 3 pots				35		
Mechanics + thin windows		15		15		
Champignons (5 in total)		15		15		
Control/electronics	15			10		
<b>GONIOMETERS</b>	<b>55</b>		<b>100</b>		<b>155</b>	<b>70</b>
Old goniometers	70					
Refurbishing of the old ones			0			
New goniometers			60			
Alignment system mechanics/electronics			20			
Control/electronics	25		20			
Near crystal detector movement	30					
<b>CRYSTALS</b>		<b>60</b>	<b>100</b>		<b>100</b>	<b>60</b>
Single/multicrystal development		30	60			
Holder		15	10			
Tests/characterization		15	30			
<b>INFRASTRUCTURE / INSTALLATION / DATA TAKING</b>	<b>230</b>	<b>139</b>	<b>100</b>	<b>59</b>	<b>528</b>	<b>195</b>
Design	60					
Cabling: existing	80					
Cabling: to be purchased	20					
Vacuum flanges and pipes	80					
Vacuum tank	35					
Infrastructure (control rooms, racks, computing)	80					
Contingency	70					
Travelling/ Per diem		139	100	59		
<b>TOTAL</b>					<b>1176</b>	<b>360</b>

Figure B.2: Detailed breakdown of the costs of the CRYSTAL experiment. The items in blue are the cost equivalent of already existing infrastructures that have to be refurbished and reconditioned or developments financed under other projects. All costs are in kCHF.



	<i>TOTAL COST (kCHF)</i>	<i>2008</i>	<i>2009</i>	<i>Cost eq.</i>
<b>CERN</b>	300	100	200	<b>+300</b>
<b>INFN</b>	326	254	72	<b>+60</b>
<b>RUSSIA</b>	300	234	66	
<b>USA</b>	250	200	50	
<b>TOTAL</b>	<b>1176</b>	<b>788</b>	<b>388</b>	<b>+360</b>

Figure B.3: Cost profile for the collaboration Institutions over the 2 years of the project.

### **B.3 Time schedule**

Fig. B.4 presents a summary schedule of the experiment. Some activities have already started: the refurbishing of the goniometer, the particle detection system development, the simulation of the setup in order to choose the ideal layout and to define the final specifications of the detectors.

Two milestones are foreseen: one in July before the start of the summer runs and one after the dry run before the organization of the installation inside the SPS ring.

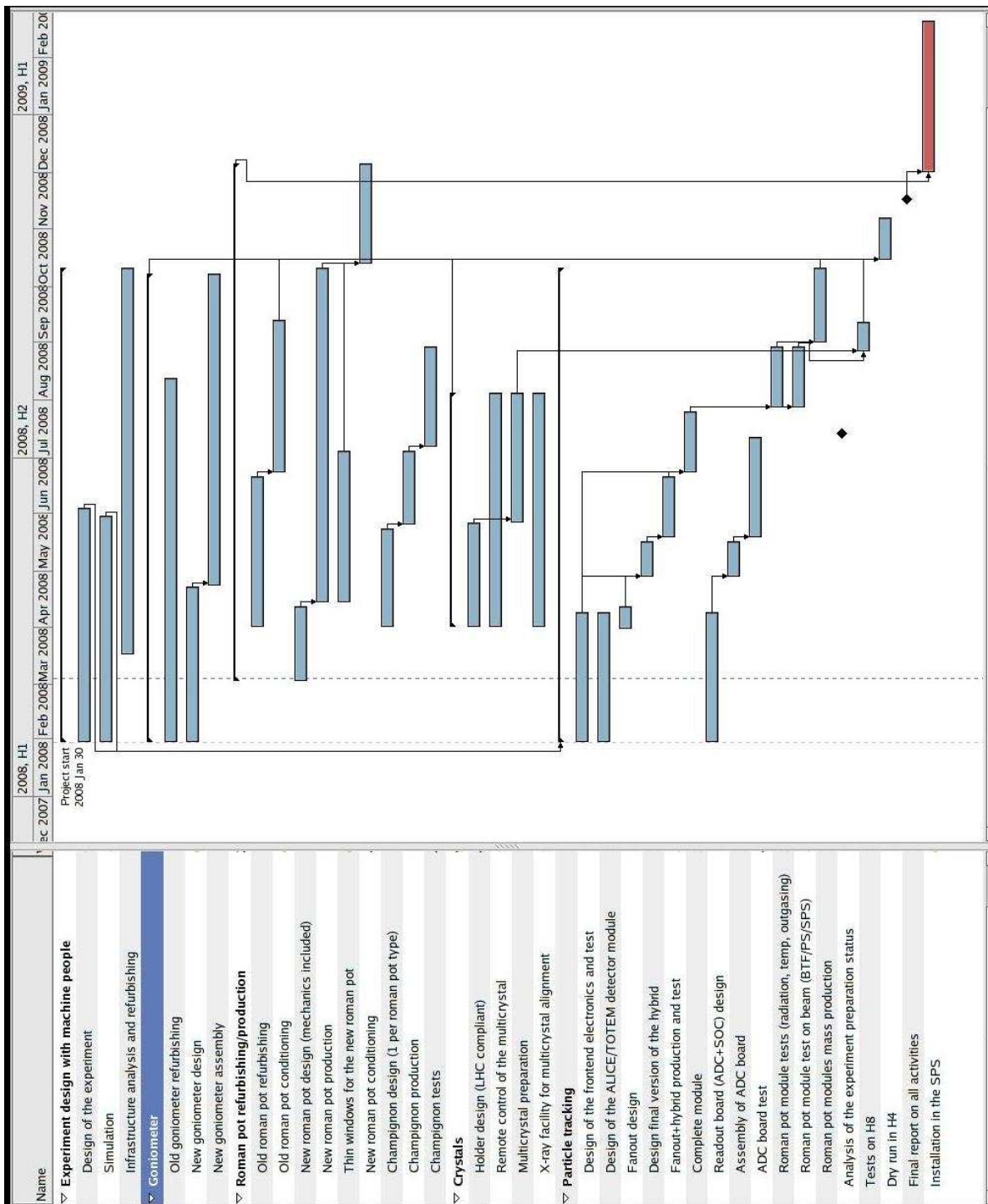


Figure B.4: Summary time schedule of the different CRYSTAL activities.

# Bibliography

- [1] J. Stark, *Phys. Zs.* 13, 973 (1912)
- [2] E. N. Tsyganov, *Fermilab reports*, TM-682 TM-684, 1979
- [3] J. Lindhard, *Phys. Lett.* 12, 126 (1964)
- [4] A. M. Taratin and S. A. Vorobiev, *Nucl. Instr. and Meth. B* 26, 512 (1987)
- [5] Y. M. Ivanov *et al.*, *JETP Letters* 84, 372 (2006)
- [6] S. I. Baker *et al.*, *Nucl. Instr. and Meth. B* 90, 119 (1994)  
C. Biino *et al.*, CERN-SL-96-30-EA (1996)  
V. M. Biryukov *et al.*, *Nucl. Instr. and Meth. B* 234, 23 (2005)
- [7] E. Uggerhoj *et al.*, *Nucl. Instr. and Meth. B* 234(1-2), 31 (2005)
- [8] A. S. Denisov *et al.*, *Nucl. Instr. and Meth. B* 69, 382 (1992)
- [9] A. Baurichter *et al.*, *Nucl. Instr. and Meth. B* 27, 164 (2000)
- [10] A. S. Bellucci *et al.*, *Phys. Rev. Lett.* 90, 034801 (2003)
- [11] A. Baurichter *et al.*, *Nucl. Instr. and Meth. B* 119, 172 (1996)
- [12] V. M. Biryukov *et al.*, *Nucl. Instr. and Meth. B* 53, 202 (1991)
- [13] R. P. Fliller, *Phys. Rev. Lett.* STA B 9, 013501 (2006)
- [14] G. Arduini *et al.*, *Phys. Rev. Lett.* 79, 4182 (1997)
- [15] K. H. Ackermann *et al.*, *Nucl. Instr. and Meth. A* 499, 624 (2003)
- [16] D. Still, *Tevatron bent crystal studies 2007*, Workshop talk: Crystal Channeling for Large Collider: Machine and Physics Application (2007)
- [17] Scandale W. *et al.*, *Phys. Rev. Lett.* 98, 154801 (2007)

- [18] Y. M. Ivanov *et al.*, Phys. Rev. Lett. 97, 144801 (2006)  
W. Scandale *et al.*, CERN/AT 2006-7, presented at the 10th EPAC'06 (2006)
- [19] W. Scandale *et al.*, Rev. Sci. Instr. 79, 023303 (2008)
- [20] W. Scandale *et al.*, Phys. Lett. B 658(4), 109 (2008)